

**Simulating snow cover in rain-on-snow event**

N. Wever et al.

# Model simulations of the modulating effect of the snow cover in a rain on snow event

N. Wever<sup>1</sup>, T. Jonas<sup>1</sup>, C. Fierz<sup>1</sup>, and M. Lehning<sup>1,2</sup>

<sup>1</sup>WSL Institute for Snow and Avalanche Research SLF, Flüelastrasse 11, 7260 Davos Dorf, Switzerland

<sup>2</sup>CRYOS, School of Architecture, Civil and Environmental Engineering, EPFL, Lausanne, Switzerland

Received: 5 March 2014 – Accepted: 30 April 2014 – Published: 15 May 2014

Correspondence to: N. Wever (wever@slf.ch)

Published by Copernicus Publications on behalf of the European Geosciences Union.

Title Page

Abstract

Introduction

Conclusions

References

Tables

Figures

⏪

⏩

◀

▶

Back

Close

Full Screen / Esc

Printer-friendly Version

Interactive Discussion



## Abstract

In October 2011, the Swiss Alps encountered a marked rain on snow event when a large snowfall on 8 and 9 October was followed by intense rain on the 10th. This resulted in severe flooding in some parts of Switzerland. Model simulations were carried out for 14 meteorological stations in two regions of the Swiss Alps using the detailed physically-based snowpack model SNOWPACK. The results show that the snow cover has a strong modulating effect on the incoming rainfall signal on the sub-daily time scales. The snowpack runoff dynamics appears to be strongly dependent on the snow depth at the onset of the rain. Deeper snow covers have more storage potential and can absorb all rain and meltwater in the first hours, whereas the snowpack runoff from shallow snow covers reacts much quicker. It has been found that after about 4–6 h, the snowpack produced runoff and after about 11–13 h, total snowpack runoff becomes higher than total rainfall as a result of additional snow melt. These values are strongly dependent on the snow height at the onset of rainfall as well as precipitation and melt rates.

An ensemble model study was carried out, in which meteorological forcing and rainfall from other stations were used for repeated simulations at a specific station. Using regression analysis, the individual contributions of rainfall, snow melt and the storage could be quantified. It was found that once the snowpack is producing runoff, deep snow covers produce more runoff than shallow ones. This could be associated with a higher contribution of the storage term. This term represents the recession curve from the liquid water storage and snowpack settling. In the event under study, snow melt in deep snow covers also turned out to be higher than in the shallow ones, although this is rather accidental.

Our results show the dual nature of snow covers in rain on snow events. Snow covers initially absorb important amounts of rain water, but once meltwater is released by the snow cover, the snowpack runoff rates strongly exceed precipitation rates due to snow melt and a contribution from the liquid water storage. This effect is stronger in

## HESSD

11, 4971–5005, 2014

### Simulating snow cover in rain-on-snow event

N. Wever et al.

[Title Page](#)

[Abstract](#)

[Introduction](#)

[Conclusions](#)

[References](#)

[Tables](#)

[Figures](#)

[⏪](#)

[⏩](#)

[◀](#)

[▶](#)

[Back](#)

[Close](#)

[Full Screen / Esc](#)

[Printer-friendly Version](#)

[Interactive Discussion](#)



deeper snow covers than in shallow ones and is probably more pronounced in rain on snow events following closely after a snowfall than for rain on snow events on spring snow. These results are specifically valid for the point scale simulations performed in this study even though field experiments are lacking to further support the model simulations. Finally, the response of catchments can be different from the response at the point scale.

## 1 Introduction

For mountain regions, the presence of a snow cover is an important factor in hydrological processes. One type of event that is still poorly understood is the behaviour of a snow cover during rainfall. These rain-on-snow (ROS) events are usually accompanied by strong snow melt, due to high latent heat exchange and incoming longwave radiation that reduces the radiative cooling of the snowpack (Marks et al., 2001; Mazurkiewicz et al., 2008). These effects increase the water available for snowpack runoff. In this way, heavy precipitation can more easily lead to flooding events in mountainous terrain due to the additional snow melt (Pradhanang et al., 2013; Sui and Koehler, 2001). Furthermore, rainfall reduces snowpack stability, resulting in stronger wet snow avalanche activity (Conway and Raymond, 1993).

Although one can estimate rather precisely how much water will be available for snowpack runoff (Marks et al., 1998; Mazurkiewicz et al., 2008), the temporal dynamics of the release of meltwater on the hourly time scale has seldomly been investigated in detail. This knowledge is essential, however, to estimate the response in streamflow discharge in catchments and to assess flood risks from ROS events.

The exact behaviour of the snow cover during ROS events is governed by complex interactions between several processes. A cold snow cover can store important amounts of rain water by capillary suction and, to a lesser extend, freezing the liquid water. These processes depend on the state of the snow cover before the onset of rain. As soon as the snow cover is getting isothermal and wet, strong settling has been

## Simulating snow cover in rain-on-snow event

N. Wever et al.

[Title Page](#)

[Abstract](#)

[Introduction](#)

[Conclusions](#)

[References](#)

[Tables](#)

[Figures](#)

[⏪](#)

[⏩](#)

[◀](#)

[▶](#)

[Back](#)

[Close](#)

[Full Screen / Esc](#)

[Printer-friendly Version](#)

[Interactive Discussion](#)



---

## Simulating snow cover in rain-on-snow event

N. Wever et al.

---

Title Page

Abstract

Introduction

Conclusions

References

Tables

Figures

◀

▶

◀

▶

Back

Close

Full Screen / Esc

Printer-friendly Version

Interactive Discussion



observed (Marshall et al., 1999). This settling, combined with a destruction of the snow matrix by melt reduces the storage capacity, which may increase snowpack runoff. These counteracting processes are difficult to assess without the use of a physically-based snow cover model. Here, the physically-based snow cover model SNOWPACK (Lehning et al., 2002b, a) is used. The SNOWPACK model has been extended recently with a solver for Richards equation, which provides a demonstrable improvement in modelling liquid water flow through the snow cover, especially on the sub-daily time scale (Wever et al., 2014).

This study focusses on the dynamical snowpack behaviour during a ROS event in October 2011 in the Swiss Alps. This event is described in detail in Badoux et al. (2013). During 8 October 2011, the passage of a cold front was bringing significant snowfall amounts on the north side of the Swiss Alps at altitudes roughly above 1000 m, accompanied by a strong drop in air temperature. During the 9th, the precipitation decayed and cold weather remained. In the night from 9 to 10 October, the passage of a warm front brought new precipitation, mainly rain, this time accompanied by a strong increase in air temperature. The snowfall limit finally increased up to 3000 m on the 10th. This ROS event is very suitable for a case study, because it was occurring on a large scale and is well captured at many measurement sites. Furthermore, the fact that it caused wide-spread flooding shows that the event was extreme in nature. One region, where the snow cover was relatively shallow, was more strongly affected by flooding than a region with a deep snow cover at the onset of rain (Badoux et al., 2013). An important question that arose from the event is whether there is a difference in snowpack behaviour for a shallow and a deep snow cover that may explain the difference in hydrological response in those two areas. The differences in streamflow response (Badoux et al., 2013), in terms of return period, would suggest that deep snowpacks can better dampen peak outflows than shallow ones.

## 2 Methods and data

### 2.1 Data

The behaviour of the snow cover in this ROS event is studied for two parts of the Swiss Alps: the Bernese Oberland and Glarner Alpen. These areas were chosen because in particular the Bernese Oberland and to a lesser extent the Glarner Alpen experienced serious flooding (Badoux et al., 2013). The studied areas are both about 1000 km<sup>2</sup>. Both areas are located on the north side of the Alps and extend more or less over a similar altitude range, with glaciated areas in the highest parts. They are about 100 km apart, and, as will be shown, have experienced different meteorological forcing conditions.

In Switzerland, about 140 automated weather stations are operational in the IMIS network. The stations measure meteorological and snow cover conditions at half hour resolution. They are equipped with wind speed and direction, temperature, relative humidity, surface temperature, soil temperature, reflected short wave radiation and snow height sensors. The stations are also equipped with an unheated rain gauge, which makes the precipitation measurements at the stations unreliable in case of snowfall. In both the Bernese Oberland and Glarner Alpen, 7 stations were selected for this study (14 in total). These stations were selected, because they are measuring at a flat measurement site, represent the altitudinal gradient in the two regions and had limited missing values during the event. The data has been quality checked manually and missing values were interpolated from neighbouring stations (Badoux et al., 2013). Most corrections were needed for wind speed, as the relatively wet snow caused the wind speed sensor to freeze at some stations. For interpreting the results, it is important to note that the average altitude of the analysed stations in the Glarner Alpen is about 270 m lower than in the Bernese Oberland.

For this study, snowfall amounts were derived from the snow height sensors at the IMIS stations, by analysing snow height changes using the SNOWPACK model (following Lehning et al., 1999). The unheated rain gauges at the IMIS stations are not

HESSD

11, 4971–5005, 2014

### Simulating snow cover in rain-on-snow event

N. Wever et al.

Title Page

Abstract

Introduction

Conclusions

References

Tables

Figures

◀

▶

◀

▶

Back

Close

Full Screen / Esc

Printer-friendly Version

Interactive Discussion



---

## Simulating snow cover in rain-on-snow event

N. Wever et al.

---

[Title Page](#)[Abstract](#)[Introduction](#)[Conclusions](#)[References](#)[Tables](#)[Figures](#)[⏪](#)[⏩](#)[◀](#)[▶](#)[Back](#)[Close](#)[Full Screen / Esc](#)[Printer-friendly Version](#)[Interactive Discussion](#)

useful during these types of events, so to estimate rainfall, a different approach was followed. The Swiss Federal Office of Meteorology and Climatology (MeteoSwiss) is operating weather stations with a heated rain gauge (ANETZ stations). Combined with several totalizers for precipitation, which are read off once per day, these precipitation measurements are compiled in a gridded dataset (RhiresD, MeteoSwiss, 2013) at 2 km resolution with daily precipitation sums (06:00–06:00 UTC). To estimate the liquid precipitation input at an IMIS station, the daily sum derived from the 9 grid points closest to the IMIS station in the RhiresD gridded data was distributed over the day by using the relative amount of precipitation registered by the closest ANETZ station. The rainfall started after 18:00 local time (LT) on 9 October and consequently, all precipitation values before this time are set to zero, as snowfall is determined from the snow height measurements.

Because the IMIS stations do not measure incoming longwave radiation, this was approximated by the Omstedt (1990) parametrisation, using an estimated cloud cover. Cloudiness was set to 1.0 in the period from 7 to 11 October, when there was either solid or liquid precipitation, and 0.5 (half cloudy) for all other times.

To validate the model performance for the chosen methods and data preparation procedures, data from the experimental site Weissfluhjoch (WFJ), located at 2540 m altitude in east Switzerland near Davos, was also used in this study. The course of the ROS event at this measurement site was quite similar to the 14 chosen IMIS stations, although both snowfall and rainfall amounts were smaller. At WFJ, both incoming and outgoing long- and shortwave radiation are available in addition to the default IMIS-type station setup, enabling a full assessment of the surface energy balance (abbreviated onwards as full EB). Furthermore, the site is equipped with a heated rain gauge that is part of the ANETZ network and a lysimeter that measures snowpack runoff (Wever et al., 2014), enabling the validation of simulated snowpack runoff.

## 2.2 SNOWPACK model

The physically-based snowpack model SNOWPACK was used to model the development of the snow cover as a 1-D-column, forced with the meteorological conditions as measured by the IMIS stations. The model simulates snow cover development, e.g. temperature and density profiles, phase changes, microstructural parameters, liquid water infiltration and snowpack runoff (Lehning et al., 2002a, b). The simulations were done using SNOWPACK version 3.2.0 in which the solver for Richards equation was introduced (Wever et al., 2014). Furthermore, improvements were made in the treatment of the boundary conditions for the energy balance and accompanying phase changes, which may explain some discrepancies with model results presented in Badoux et al. (2013).

The model was forced to interpret increases in snow height as snowfall, deriving the new snow density from a parametrised relationship between wind speed, temperature and relative humidity (Schmucki et al., 2014). A temperature threshold of  $0.0^{\circ}\text{C}$  is used to determine whether precipitation should be considered rain (from RhiresD) or snow (from the snow height sensor). This threshold is determined by comparing the ventilated and unventilated temperature sensor at WFJ during this particular event. It was found that when the ventilated sensor was close to  $1.2^{\circ}\text{C}$ , the unventilated IMIS type sensor was measuring around  $0.0^{\circ}\text{C}$ .

Snow melt is an important source of liquid water in the snowpack. In the SNOWPACK model, snow melt occurs at a specific depth when the local temperature is  $0^{\circ}\text{C}$  and excess energy is added at this depth after solving the heat advection equation for the snowpack and soil continuum. At the top of the snowpack, the model prescribes the energy flux as a Neumann boundary condition in case of melting conditions in the top snow element or else as a Dirichlet boundary condition, prescribing the measured snow surface temperature. The latter ensures a better assessment of the cold content of the snowpack, although it may result in numerical discrepancies in the energy balance.

## HESSD

11, 4971–5005, 2014

### Simulating snow cover in rain-on-snow event

N. Wever et al.

[Title Page](#)

[Abstract](#)

[Introduction](#)

[Conclusions](#)

[References](#)

[Tables](#)

[Figures](#)

[⏪](#)

[⏩](#)

[◀](#)

[▶](#)

[Back](#)

[Close](#)

[Full Screen / Esc](#)

[Printer-friendly Version](#)

[Interactive Discussion](#)



## Simulating snow cover in rain-on-snow event

N. Wever et al.

Title Page

Abstract

Introduction

Conclusions

References

Tables

Figures

⏪

⏩

◀

▶

Back

Close

Full Screen / Esc

Printer-friendly Version

Interactive Discussion



The heat flux at the top of the snowpack can be expressed as (Lehning et al., 2002a):

$$Q_{\text{sum}} = R_{\text{net}} + Q_{\text{S}} + Q_{\text{L}} + Q_{\text{P}} \quad (1)$$

where  $Q_{\text{sum}}$  is the prescribed flux ( $\text{Wm}^{-2}$ ),  $R_{\text{net}}$  is the net radiation ( $\text{Wm}^{-2}$ ),  $Q_{\text{S}}$  is the sensible heat ( $\text{Wm}^{-2}$ ),  $Q_{\text{L}}$  is the latent heat ( $\text{Wm}^{-2}$ ) and  $Q_{\text{P}}$  is the heat advection by liquid precipitation ( $\text{Wm}^{-2}$ ). For calculating the fluxes, a neutral atmospheric stratification was assumed, which is likely an appropriate assumption because of the windy conditions during the event. The shortwave radiation input is actually not incorporated in the Neumann boundary condition for the temperature equation, but is used as a source term in the top layers of the snowpack to reflect the penetration of shortwave radiation in the snowpack. The turbulent heat fluxes are calculated following a standard Monin–Obukhov parametrisation (Lehning et al., 2002b), using a roughness length  $z_0$  of 0.002 m. The net radiation is approximated by using the measured reflected shortwave radiation and a parametrised albedo (Schmucki et al., 2014).

Water transport in snow is governed by capillary suction and gravitational drainage (Marsh, 2006). Two common model approaches for liquid water flow in snow are the so-called bucket scheme and Richards equation (Wever et al., 2014). In the bucket scheme, downward water transport is determined by the presence of an excess liquid water content above a defined threshold water content in a specific layer. This excess water is transported downward regardless of the storage capacity of lower layers. In Richards equation, the balance between gravitation and capillary suction is explicitly calculated. It yields performance improvement over the bucket approach on both daily and hourly time scales (Wever et al., 2014). However, solving Richards equation may be expected to especially improve the simulation of water flow in seasonal snow covers, where snow stratigraphy can have a marked influence on the water flow. Differences in grain sizes can lead to capillary barriers and ice lenses may block the water flow, resulting in ponding (Marsh, 1999; Hirashima et al., 2010). For this ROS event, the snow cover built up in two days, leading to a very homogeneous stratification.



in the snow cover is not clear a priori. Note that altitudinal differences between the stations in both regions make a direct comparison between the two regions difficult. However, the analysis of those 4 variables implicitly captures the altitudinal gradients.

To investigate the factors influencing the response of the snow cover during the ROS event, we also forced the SNOWPACK model for each station with the meteorological conditions from the other stations. For example: snow melt is mainly governed by meteorological conditions and liquid precipitation has relatively little impact. So the meteorological forcing, excluding the liquid precipitation, at the 14 stations represent 14 different melt scenarios. For liquid precipitation, we also have 14 more or less unique scenarios, although the temporal distribution over the day is based on 8 ANETZ stations only. However, the scenarios provide differences in rainfall amounts due to the spatial distribution as captured in the RhiresD dataset by spatial interpolations and climatological lapse rates. So for each of the 14 stations, with its own unique maximum snow height, we performed an ensemble of  $13 \times 13 = 169$  additional simulations with the SNOWPACK model, with every combination of melt and precipitation scenario for statistical analysis. For these simulations, the original meteorological measurements at the stations were used to force the model up to the moment on which the rainfall started at the stations on 9 October. From this specific time onwards, the meteorological forcing and precipitation was replaced by forcings from other stations, starting at the date and time when rainfall started at these other stations.

To analyse possible different effects on snowpack runoff for shallow and deep snow covers, the 14 IMIS stations were divided in a shallow and a deep snow cover class, depending on being above or below the median of maximum snow height during the event. The stations in Bernese Oberland are all present in the shallow snow cover class, except for GAN2 and all stations in Glarner Alpen are in the deep snow cover class, except SCA2. Per class, we determined the linear regression for a given cumulative period using all ensemble simulations in the respective class:

$$Q_{\text{cum}} = \alpha P_{\text{cum}} + \beta M_{\text{cum}} + b, \quad (2)$$

## HESSD

11, 4971–5005, 2014

### Simulating snow cover in rain-on-snow event

N. Wever et al.

Title Page

Abstract

Introduction

Conclusions

References

Tables

Figures

◀

▶

◀

▶

Back

Close

Full Screen / Esc

Printer-friendly Version

Interactive Discussion



where  $Q_{\text{cum}}$  is the cumulative snowpack runoff sum (mm w.e.),  $P_{\text{cum}}$  is the cumulative precipitation sum (mm),  $\alpha$  is the linear regression coefficient for precipitation,  $M_{\text{cum}}$  is the cumulative snow melt sum (mm w.e.),  $\beta$  is the linear regression coefficient for snow melt and  $b$  is the intercept. Note that in this context,  $b$  can be interpreted as the change in liquid water storage in the snow cover. As a positive value of  $b$  describes the snowpack runoff in the absence of any rain or snow melt, it can be assumed to reflect the recession curve and the settling effect.

The dependence of the fit coefficients  $\alpha$ ,  $\beta$  and  $b$  over varying cumulative periods can reveal how the snow cover is modulating precipitation input and snow melt. These coefficients will be used on the original simulations to attribute the individual contributions of snow melt, precipitation and the intercept (change in storage) to the modelled snowpack runoff. The linear regression was done for cumulative periods of 0–1 to 0–24 h with two approaches: (i) taking the onset of rain at the stations as the start of the cumulative period and (ii) taking the onset of snowpack runoff as the start of the cumulative period. The latter was determined by both an increase of snowpack runoff by a factor 2 compared to the snowpack runoff at the onset of rain and a modelled snowpack runoff larger than 0.5 mm in 15 min.

### 3 Results and discussion

#### 3.1 Verification

Before discussing the simulations for the two study regions, the results for the verification station WFJ will be presented. Figure 1 shows the modelled and measured snowpack runoff for the ROS event, starting shortly before the onset of rain for the WFJ measurement site. The figure shows that solving liquid water flow in the snow cover with Richards equation is providing a closer agreement with observed snowpack runoff than with the bucket scheme concerning the timing of snowpack runoff. Both models are overestimating the snowpack runoff, as shown by the steeper cumulative curve,

## Simulating snow cover in rain-on-snow event

N. Wever et al.

Title Page

Abstract

Introduction

Conclusions

References

Tables

Figures

⏪

⏩

◀

▶

Back

Close

Full Screen / Esc

Printer-friendly Version

Interactive Discussion



although the overestimation is larger with the bucket scheme. Because of the focus on snowpack runoff in this study, all further calculations will be done with Richards equation only. It should be noted however, that several parametrisations are not yet verified with Richards equation (like metamorphism, snow settling, etc).

In spite of some differences between the full energy balance station from WFJ and the IMIS-type setup from WFJ, it can be seen that the approach of parametrising ILWR and deriving precipitation from the RhiresD data and the ANETZ stations is providing reasonable results. It shows that the methods used in this study are suitable for analysing the dynamical snowpack behaviour at the IMIS stations in the two study areas. It should be noted however, that the timing of precipitation for WFJ is very accurate, because a heated ANETZ rain gauge is located at this site, whereas for other stations, the closest ANETZ stations is several kilometres away.

### 3.2 Event description

The event started with snowfall above roughly 1000 m altitude on 7 October. Figure 2 shows the temporal development of snow cover height in the two study regions. As can be seen, the snowfall was quite continuous and the maximum snow height averaged over all stations was reached around 9 October, 12:00 LT. Table 1 shows that the average maximum snow height at the 7 IMIS stations in Bernese Oberland was 57 cm, less than the 92 cm in the Glarner Alpen. In Bernese Oberland, snow fall amounts tend to increase with altitude, whereas interestingly, this trend is absent in the Glarner Alpen.

After the maximum snow height has been reached, the snow height starts decreasing, although rain and surface snow melt have not started yet. This decrease can be attributed mainly to settling of the snowpack and basal melt by the ground heat flux. The following precipitation event started after 18:00 LT on 9 October, and consisted purely of rainfall (except for very high altitudes). It was accompanied by a rapid increase of the 0 °C-isotherm to 3000 m altitude. The rainfall lasted until 15:00 LT on 10 October,

## Simulating snow cover in rain-on-snow event

N. Wever et al.

Title Page

Abstract

Introduction

Conclusions

References

Tables

Figures

◀

▶

◀

▶

Back

Close

Full Screen / Esc

Printer-friendly Version

Interactive Discussion





stored additionally in the snow cover by capillary suction. The shallow snow cover at the stations in the Bernese Oberland could retain less meltwater than the deeper snow cover at the stations in Glarner Alpen. Furthermore, the tipping point where a net storage of liquid water in the snow cover changed into a net release of liquid water from the snow cover, was reached earlier in Bernese Oberland (4 h) than in Glarner Alpen (7 h). Table 1 also shows the time needed before cumulative snowpack runoff exceeded cumulative rainfall, which is generally shorter in Bernese Oberland than in Glarner Alpen. However, it still took on average 11–13 h since the start of rainfall before the total snowpack runoff exceeded total rainfall. This shows that the dampening effect of the rainfall by the snow cover is quite strong and persists for several hours. Figure 4 also shows a wide spread between individual stations, related to variations in rainfall and snow melt rates. This motivates to carry out the ensemble simulations that will be discussed later.

### 3.3 Energy balance

A net positive energy balance for the surface will first result in a heating of the snowpack (reducing the cold content), followed by melt. Table 2 shows the energy balance at the stations, expressed as mmw.e. melt potential as if the energy would be solely used for snow melt or freezing, the latter resulting in warming of the snow cover. The time period denoted as “Event” in Tables 1 and 2 is arbitrarily chosen to contain at least the complete rainfall, but longer or shorter time periods may have a significant effect on the relative contribution of the terms. A comparison with the amount of snow melt provided in Table 1 reveals that at all stations, most energy was used for snow melt. For stations with a high cold content, the net energy is partly used for heating of the snowpack. The contribution of net radiative energy, if not negative, and rain energy is fairly small. Most energy was delivered by heat release due to condensation during the ROS event and sensible heat. Mazurkiewicz et al. (2008) also found a strong contribution of latent heat to snow melt during ROS events. This is in contrast with typical clear sky spring snow melt situations, where both terms often have opposite sign (Mott et al., 2013). Note that

## Simulating snow cover in rain-on-snow event

N. Wever et al.

Title Page

Abstract

Introduction

Conclusions

References

Tables

Figures

◀

▶

◀

▶

Back

Close

Full Screen / Esc

Printer-friendly Version

Interactive Discussion





concluded that the formation of efficient preferential flow paths (not considered in the SNOWPACK model) is likely contributing to this high average velocity.

#### 4.1 Regression analysis

The regression analysis (Eq. 2) was carried out to investigate the influence of the different mechanisms in producing snowpack runoff. Figure 7a shows the regression coefficients for both the shallow and deep snow cover class as a function of cumulative period since the start of rain. The figure shows that in the shallow snow cover class, rain is correlated to snowpack runoff after 2 h already, whereas in the deep snow cover class, the first non zero regression coefficient is found after 5 h. Furthermore, the coefficient for snow melt is higher in the shallow snow cover class than in the deep one. This is caused by the larger time lag between the onset of rain and the onset of snowpack runoff in the deep snow cover class. It should be noted that the snow melt in the first hours after the onset of rain is for a significant part due to basal melt and is therefore correlating with snowpack runoff without a time lag.

At the 24 h cumulative period after the start of rain, there is no difference in regression coefficient for melt and rain between the shallow and deep snow cover class. Interestingly, the coefficient for rain is almost equal to 1.0, whereas the coefficient for melt is about 1.1. The latter suggests that there is approximately 10% extra snowpack runoff due to snow melt as a result of the destruction of the snow matrix. The intercept term clearly shows that the deep snow covers have more storage capacity for meltwater, which results in a longer delay between the onset of rain and the actual snowpack runoff.

In Fig. 7b, the regression coefficients are shown for cumulative periods starting at the onset of snowpack runoff. Expectedly, the intercept term changes sign: once snowpack runoff is starting, there is a contribution from the intercept. This contribution consists of the snow melt and precipitation prior to the onset of snowpack runoff. Furthermore, settling may cause a reduction in storage capacity of the snow cover.

## Simulating snow cover in rain-on-snow event

N. Wever et al.

[Title Page](#)

[Abstract](#)

[Introduction](#)

[Conclusions](#)

[References](#)

[Tables](#)

[Figures](#)

[⏪](#)

[⏩](#)

[◀](#)

[▶](#)

[Back](#)

[Close](#)

[Full Screen / Esc](#)

[Printer-friendly Version](#)

[Interactive Discussion](#)





class than in the shallow one. This clearly illustrates a higher snowpack runoff in the deep snow cover class once snowpack runoff starts. To assess the relationship with snow cover depth, Fig. 9 shows the snowpack runoff sums in the first hours after the start of snowpack runoff and the maximum peak snowpack runoff sum over the first 24 h after the onset of rain, averaged over all 169 simulations per individual station (associated with a specific snow depth). As can be seen, the snowpack runoff in the first hours shows a clear increase with snow depth, whereas the trend is much smaller for the maximum snowpack runoff. The reason for this is likely that the maximum peak snowpack runoff is achieved in a kind of steady state situation when incoming rainfall and snow melt is in balance with snowpack runoff. The fact that this value is almost constant with snow depth, is a consequence of the ensemble simulation setup, where all precipitation and melt scenarios are present for each station.

The simulations suggest that deep snow covers initially produce more snowpack runoff than shallow snow covers and that this effect is partly caused by hydraulic effects inside the snowpack and partly by higher snow melt amounts. In Fig. 10a and b, the percentages of respectively intercept, snow melt and rainfall contributions to snowpack runoff are shown for increasing cumulative periods, as determined by the regression analysis. These figures confirm the earlier conclusions. The contribution of the storage is varying between 15 and 20% and is higher in the deep snow cover class. The contribution of snow melt is almost doubling from 15 and 20% to 30 and 38% between 1 and 24 h cumulative periods for the shallow and deep snow covers, respectively. It should be noted that the higher amount of snow melt experienced at the stations in the deeper snow cover class is rather accidental, whereas the higher contribution of the intercept term for the deeper snow cover class is truly connected to the deeper snow cover.

## HESSD

11, 4971–5005, 2014

### Simulating snow cover in rain-on-snow event

N. Wever et al.

[Title Page](#)

[Abstract](#)

[Introduction](#)

[Conclusions](#)

[References](#)

[Tables](#)

[Figures](#)

[⏪](#)

[⏩](#)

[◀](#)

[▶](#)

[Back](#)

[Close](#)

[Full Screen / Esc](#)

[Printer-friendly Version](#)

[Interactive Discussion](#)



## 5 Conclusions

Model simulations of a ROS event in October 2011 for 14 meteorological stations in two regions of the Swiss Alps have shown that the snowpack runoff dynamics from the snow cover is strongly dependent on the snow depth at the onset of the rain. Deeper snow covers have more storage and absorb all rain and meltwater in the first hours, whereas the snowpack runoff from shallow snow covers reacts much quicker to the onset of rainfall. It was found that (for this event) after on average 11–13 h, cumulative snowpack runoff becomes higher than cumulative rainfall as a result of additional snow melt.

An ensemble of simulations was carried out where meteorological and precipitation forcing conditions were interchanged for each station. It was found that the time lag between the onset of rainfall and snowpack runoff in the model study depends on snow height as well as the sum of rainfall and melt rates. A regression analysis on the ensemble simulations has shown that deep snow covers generate more runoff, once meltwater is leaving the snowpack. The results suggest that this is caused by a higher contribution of released liquid water storage than in shallow snow covers. The storage contains water previously stored in the snowpack and changes therein reflect both snowpack settling and the recession curve from the storage. Furthermore, the region in this study with mainly deep snow covers (Glarner Alpen) was having more snow melt during this event. It was crucial for the event that also in the deep snow cover class, the amount of rainfall and snow melt was largely exceeding the storage capacity of the snow and, as a consequence, significant amounts of snowpack runoff were generated. The differences between deep and shallow snow covers in ROS events on spring snow, where most settling has already occurred and liquid water is already present in the snowpack, are expected to be less pronounced.

Given that the snow cover was deeper in Glarner Alpen than in Bernese Oberland, these differences in snowpack behaviour in terms of time lag between the onset of rain and the onset of snowpack runoff may have contributed to the differences found

**HESSD**

11, 4971–5005, 2014

### Simulating snow cover in rain-on-snow event

N. Wever et al.

[Title Page](#)

[Abstract](#)

[Introduction](#)

[Conclusions](#)

[References](#)

[Tables](#)

[Figures](#)

[⏪](#)

[⏩](#)

[◀](#)

[▶](#)

[Back](#)

[Close](#)

[Full Screen / Esc](#)

[Printer-friendly Version](#)

[Interactive Discussion](#)





## Simulating snow cover in rain-on-snow event

N. Wever et al.

Title Page

Abstract

Introduction

Conclusions

References

Tables

Figures

◀

▶

◀

▶

Back

Close

Full Screen / Esc

Printer-friendly Version

Interactive Discussion



- Calonne, N., Geindreau, C., Flin, F., Morin, S., Lesaffre, B., Rolland du Roscoat, S., and Charrier, P.: 3-D image-based numerical computations of snow permeability: links to specific surface area, density, and microstructural anisotropy, *The Cryosphere*, 6, 939–951, doi:10.5194/tc-6-939-2012, 2012. 4979
- 5 Conway, H. and Raymond, C. F.: Snow stability during rain, *J. Glaciol.*, 39, 635–642, 1993. 4973
- Hirashima, H., Yamaguchi, S., Sato, A., and Lehning, M.: Numerical modeling of liquid water movement through layered snow based on new measurements of the water retention curve, *Cold Reg. Sci. Technol.*, 64, 94–103, doi:10.1016/j.coldregions.2010.09.003, 2010. 4978
- 10 Jordan, P.: Meltwater movement in a deep snowpack: 1. Field observations, *Water Resour. Res.*, 19, 971–978, doi:10.1029/WR019i004p00971, 1983. 4985
- Lehning, M., Bartelt, P., Brown, B., Russi, T., Stöckli, U., and Zimmerli, M.: SNOWPACK calculations for avalanche warning based upon a new network of weather and snow stations, *Cold Reg. Sci. Technol.*, 30, 145–157, doi:10.1016/S0165-232X(99)00022-1, 1999. 4975
- 15 Lehning, M., Bartelt, P., Brown, B., and Fierz, C.: A physical SNOWPACK model for the Swiss avalanche warning Part III: Meteorological forcing, thin layer formation and evaluation, *Cold Reg. Sci. Technol.*, 35, 169–184, doi:10.1016/S0165-232X(02)00072-1, 2002a. 4974, 4977, 4978
- Lehning, M., Bartelt, P., Brown, B., Fierz, C., and Satyawali, P.: A physical SNOWPACK model for the Swiss avalanche warning Part II: Snow microstructure, *Cold Reg. Sci. Technol.*, 35, 147–167, doi:10.1016/S0165-232X(02)00073-3, 2002b. 4974, 4977, 4978
- 20 Marks, D., Kimball, J., Tingey, D., and Link, T.: The sensitivity of snowmelt processes to climate conditions and forest cover during rain-on-snow: a case study of the 1996 Pacific Northwest flood, *Hydrol. Process.*, 12, 1569–1587, doi:10.1002/(SICI)1099-1085(199808/09)12:10<1569::AID-HYP682>3.0.CO;2-L, 1998. 4973
- 25 Marks, D., Link, T., Winstral, A., and Garen, D.: Simulating snowmelt processes during rain-on-snow over a semi-arid mountain basin, *Ann. Glaciol.*, 32, 195–202, doi:10.3189/172756401781819751, 2001. 4973
- Marsh, P.: Snowcover formation and melt: recent advances and future prospects, *Hydrol. Process.*, 13, 2117–2134, doi:10.1002/(SICI)1099-1085(199910)13:14/15<2117::AID-HYP869>3.0.CO;2-9, 1999. 4978
- 30

## Simulating snow cover in rain-on-snow event

N. Wever et al.

Title Page

Abstract

Introduction

Conclusions

References

Tables

Figures

◀

▶

◀

▶

Back

Close

Full Screen / Esc

Printer-friendly Version

Interactive Discussion



Marsh, P.: Water flow through snow and firn, in: Encyclopedia of Hydrological Sciences, John Wiley & Sons Ltd., Chichester, England, chap. 161, 1–14, doi:10.1002/0470848944.hsa167, 2006. 4978

Marshall, H., Conway, H., and Rasmussen, L.: Snow densification during rain, Cold Reg. Sci. Technol., 30, 35–41, doi:10.1016/S0165-232X(99)00011-7, 1999. 4974

Mazurkiewicz, A. B., Callery, D. G., and McDonnell, J. J.: Assessing the controls of the snow energy balance and water available for runoff in a rain-on-snow environment, J. Hydrol., 354, 1–14, doi:10.1016/j.jhydrol.2007.12.027, 2008. 4973, 4984

MeteoSwiss: Documentation of MeteoSwiss Grid-Data Products, Daily Precipitation (final analysis): RhiresD, Tech. rep., Federal Office of Meteorology and Climatology MeteoSwiss, Zürich, Switzerland, 2013. 4976

Mott, R., Gromke, C., Grünewald, T., and Lehning, M.: Relative importance of advective heat transport and boundary layer decoupling in the melt dynamics of a patchy snow cover, Adv. Water Resour., 55, 88–97, doi:10.1016/j.advwatres.2012.03.001, 2013. 4984

Omstedt, A.: A coupled one-dimensional sea ice-ocean model applied to a semi-enclosed basin, Tellus A, 42, 568–582, doi:10.1034/j.1600-0870.1990.t01-3-00007.x, 1990. 4976

Pradhanang, S. M., Frei, A., Zion, M., Schneiderman, E. M., Steenhuis, T. S., and Pierson, D.: Rain-on-snow runoff events in New York, Hydrol. Process., 27, 3035–3049, doi:10.1002/hyp.9864, 2013. 4973

Schmucki, E., Marty, C., Fierz, C., and Lehning, M.: Evaluation of modelled snow depth and snow water equivalent at three contrasting sites in Switzerland using SNOWPACK simulations driven by different meteorological data input, Cold Reg. Sci. Technol., 99, 27–37, doi:10.1016/j.coldregions.2013.12.004, 2014. 4977, 4978

Singh, P., Spitzbart, G., Hübl, H., and Weinmeister, H.: Hydrological response of snowpack under rain-on-snow events: a field study, J. Hydrol., 202, 1–20, doi:10.1016/S0022-1694(97)00004-8, 1997. 4985

Sui, J. and Koehler, G.: Rain-on-snow induced flood events in Southern Germany, J. Hydrol., 252, 205–220, doi:10.1016/S0022-1694(01)00460-7, 2001. 4973

Wever, N., Fierz, C., Mitterer, C., Hirashima, H., and Lehning, M.: Solving Richards Equation for snow improves snowpack meltwater runoff estimations in detailed multi-layer snowpack model, The Cryosphere, 8, 257–274, doi:10.5194/tc-8-257-2014, 2014. 4974, 4976, 4977, 4978, 4979

Yamaguchi, S., Katsushima, T., Sato, A., and Kumakura, T.: Water retention curve of snow with different grain sizes, Cold Reg. Sci. Technol., 64, 87–93, doi:10.1016/j.coldregions.2010.05.008, 2010. 4979

# HESSD

11, 4971–5005, 2014

## Simulating snow cover in rain-on-snow event

N. Wever et al.

[Title Page](#)

[Abstract](#)

[Introduction](#)

[Conclusions](#)

[References](#)

[Tables](#)

[Figures](#)

[|◀](#)

[▶|](#)

[◀](#)

[▶](#)

[Back](#)

[Close](#)

[Full Screen / Esc](#)

[Printer-friendly Version](#)

[Interactive Discussion](#)



## Simulating snow cover in rain-on-snow event

N. Wever et al.

**Table 1.** List of station abbreviations, station names, station altitudes and statistics for the two study areas and the verification station. The statistics denoted with Event are determined over the period 9 October, 18:00LT–11 October, 00:00LT. Time lag is the lag between the start of rain and the start of snowpack runoff and time runoff > rain denotes the time it took before cumulative snowpack runoff exceeded cumulative rainfall.

| stn                  | name          | altitude<br>(m) | max snow height<br>6–14 Oct<br>(cm) | rainfall<br>Event<br>(mm) | deposition<br>Event<br>(mm w.e.) | snowmelt<br>Event<br>(mmp w.e.) | snowpack runoff<br>Event<br>(mm w.e.) | cold content<br>(kJm <sup>3</sup> ) | time lag<br>(hours) | time runoff > rain<br>(hours) |
|----------------------|---------------|-----------------|-------------------------------------|---------------------------|----------------------------------|---------------------------------|---------------------------------------|-------------------------------------|---------------------|-------------------------------|
| Bernese Oberland     |               |                 |                                     |                           |                                  |                                 |                                       |                                     |                     |                               |
| FAE2                 | Faermel       | 1970            | 39                                  | 63                        | 1.0                              | 29                              | 97                                    | 26                                  | 2.2                 | 4.8                           |
| ELS2                 | Elsige        | 2140            | 44                                  | 59                        | 1.3                              | 34                              | 94                                    | 33                                  | 3.5                 | 6.2                           |
| MUN2                 | Mund          | 2210            | 53                                  | 34                        | 2.0                              | 45                              | 81                                    | 8                                   | 2.2                 | 6.2                           |
| SCH2                 | Schilthorn    | 2360            | 70                                  | 88                        | 0.5                              | 14                              | 95                                    | 387                                 | 4.8                 | 19.5                          |
| TRU2                 | Trubelboden   | 2480            | 37                                  | 84                        | 0.8                              | 22                              | 106                                   | 60                                  | 3.8                 | 9.8                           |
| BEL2                 | Belalp        | 2556            | 51                                  | 43                        | 0.2                              | 5                               | 44                                    | 161                                 | 3.0                 | 18.0                          |
| GAN2                 | Gandegg       | 2717            | 103                                 | 75                        | 0.4                              | 2                               | 63                                    | 1263                                | 10.0                | –                             |
| average all          |               | 2348            | 57                                  | 64                        | 0.9                              | 22                              | 83                                    | 277                                 | 4.2                 | 10.8                          |
| Glarner Alpen        |               |                 |                                     |                           |                                  |                                 |                                       |                                     |                     |                               |
| GLA2                 | Glaernisch    | 1630            | 99                                  | 72                        | 0.7                              | 36                              | 98                                    | 272                                 | 7.2                 | 14.5                          |
| ORT2                 | Ortstock      | 1830            | 108                                 | 76                        | 3.8                              | 70                              | 142                                   | 798                                 | 7.5                 | 12.5                          |
| SCA2                 | Schächental   | 2030            | 73                                  | 75                        | 2.5                              | 71                              | 146                                   | 330                                 | 5.5                 | 9.8                           |
| ELM2                 | Elm           | 2050            | 90                                  | 53                        | 1.0                              | 24                              | 67                                    | 559                                 | 5.2                 | 13.0                          |
| TUM2                 | Tumpiv        | 2195            | 93                                  | 41                        | 0.6                              | 33                              | 67                                    | 662                                 | 5.0                 | 10.8                          |
| SCA3                 | Schächental   | 2330            | 90                                  | 81                        | 1.6                              | 23                              | 95                                    | 972                                 | 5.2                 | 14.8                          |
| MUT2                 | Muttsee       | 2474            | 92                                  | 63                        | 0.7                              | 10                              | 61                                    | 929                                 | 7.0                 | –                             |
| average all          |               | 2077            | 92                                  | 66                        | 1.5                              | 38                              | 96                                    | 646                                 | 6.1                 | 12.5                          |
| Verification station |               |                 |                                     |                           |                                  |                                 |                                       |                                     |                     |                               |
| WFJ                  | Weissfluhjoch | 2540            | 48                                  | 33                        | 1.1                              | 18                              | 47                                    | 811                                 | 4.8                 | 11.2                          |

Title Page

Abstract

Introduction

Conclusions

References

Tables

Figures

⏪

⏩

◀

▶

Back

Close

Full Screen / Esc

Printer-friendly Version

Interactive Discussion



## Simulating snow cover in rain-on-snow event

N. Wever et al.

**Table 2.** Energy balance at the stations for the period 9 October, 18:00LT–11 October, 00:00LT. The energy fluxes are expressed as an equivalent snow melt energy in mm w.e. for understanding the magnitude of the energy fluxes, although snow melt should not necessarily have occurred.

| stn                  | altitude (m) | Rnet (mm w.e.) | rain energy (mm w.e.) | latent heat flux (mm w.e.) | sensible heat flux (mm w.e.) | soil heat flux (mm w.e.) | total energy (mm w.e.) |
|----------------------|--------------|----------------|-----------------------|----------------------------|------------------------------|--------------------------|------------------------|
| Bernese Oberland     |              |                |                       |                            |                              |                          |                        |
| FAE2                 | 1970         | 1              | 5                     | 8                          | 9                            | 6                        | 28                     |
| ELS2                 | 2140         | -1             | 4                     | 10                         | 12                           | 5                        | 30                     |
| MUN2                 | 2210         | -3             | 1                     | 17                         | 22                           | 4                        | 41                     |
| SCH2                 | 2360         | -3             | 4                     | 4                          | 8                            | 1                        | 14                     |
| TRU2                 | 2480         | -2             | 6                     | 6                          | 15                           | -0                       | 24                     |
| BEL2                 | 2556         | -5             | 1                     | 1                          | 3                            | 1                        | 1                      |
| GAN2                 | 2717         | -6             | 1                     | 3                          | 6                            | 0                        | 5                      |
| average all          | 2348         | -3             | 3                     | 7                          | 11                           | 2                        | 20                     |
| Glarner Alpen        |              |                |                       |                            |                              |                          |                        |
| GLA2                 | 1630         | 2              | 6                     | 5                          | 8                            | 11                       | 31                     |
| ORT2                 | 1830         | -0             | 6                     | 30                         | 37                           | 12                       | 85                     |
| SCA2                 | 2030         | -1             | 6                     | 18                         | 38                           | 6                        | 69                     |
| ELM2                 | 2050         | -1             | 3                     | 7                          | 7                            | 6                        | 22                     |
| TUM2                 | 2195         | -0             | 3                     | 4                          | 13                           | 11                       | 32                     |
| SCA3                 | 2330         | -4             | 3                     | 12                         | 13                           | 1                        | 25                     |
| MUT2                 | 2474         | -6             | 1                     | 5                          | 8                            | 1                        | 10                     |
| average all          | 2077         | -1             | 4                     | 12                         | 18                           | 7                        | 39                     |
| Verification station |              |                |                       |                            |                              |                          |                        |
| WFJ                  | 2540         | -6             | 0                     | 8                          | 14                           | 0                        | 17                     |

Title Page

Abstract Introduction

Conclusions References

Tables Figures

⏪ ⏩

◀ ▶

Back Close

Full Screen / Esc

Printer-friendly Version

Interactive Discussion



## Simulating snow cover in rain-on-snow event

N. Wever et al.

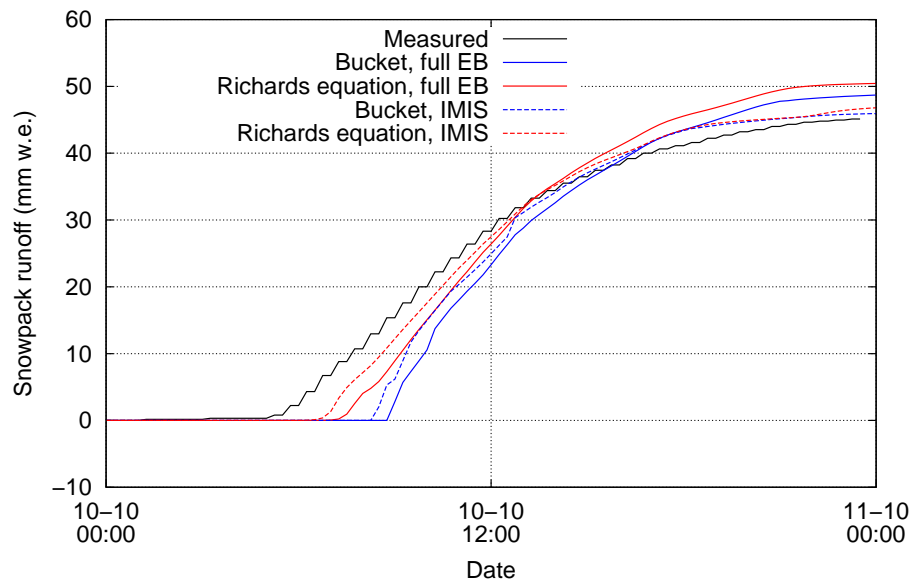


**Fig. 1.** Comparison of modelled snowpack runoff using the bucket scheme or Richards equation for liquid water transport in the snowpack with measured snowpack runoff by a lysimeter for the station Weissfluhjoch, for 10 October. Simulations are done with either the full energy balance meteorological forcing (solid lines), or with the forcing available for IMIS-type stations (dashed lines).

[Title Page](#)[Abstract](#)[Introduction](#)[Conclusions](#)[References](#)[Tables](#)[Figures](#)[◀](#)[▶](#)[◀](#)[▶](#)[Back](#)[Close](#)[Full Screen / Esc](#)[Printer-friendly Version](#)[Interactive Discussion](#)

## Simulating snow cover in rain-on-snow event

N. Wever et al.

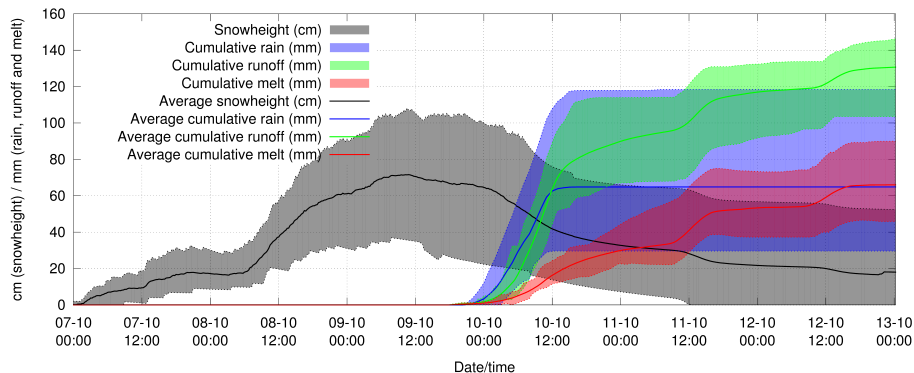


**Fig. 2.** Overview of the simulation results of the temporal evolution of the ROS event between 7 and 13 October. Shown is the range of absolute minimum and maximum modelled snow height, cumulative precipitation, cumulative snowpack runoff and cumulative melt over the 14 stations. The solid lines denote the average values. The accumulation for precipitation and melt was calculated from 9 October, 18:00 LT onwards.

Title Page

Abstract

Introduction

Conclusions

References

Tables

Figures

◀

▶

◀

▶

Back

Close

Full Screen / Esc

Printer-friendly Version

Interactive Discussion



## Simulating snow cover in rain-on-snow event

N. Wever et al.

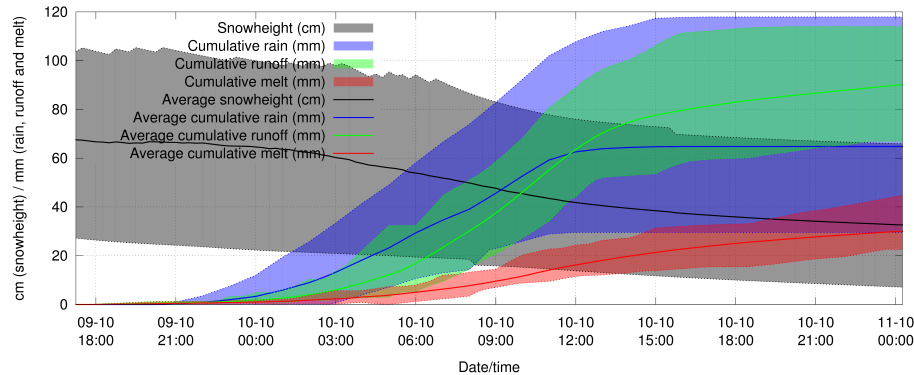


**Fig. 3.** Detail of Fig. 2, showing the main ROS event.

[Title Page](#)

[Abstract](#) | [Introduction](#)

[Conclusions](#) | [References](#)

[Tables](#) | [Figures](#)

[⏪](#) | [⏩](#)

[◀](#) | [▶](#)

[Back](#) | [Close](#)

[Full Screen / Esc](#)

[Printer-friendly Version](#)

[Interactive Discussion](#)



## Simulating snow cover in rain-on-snow event

N. Wever et al.

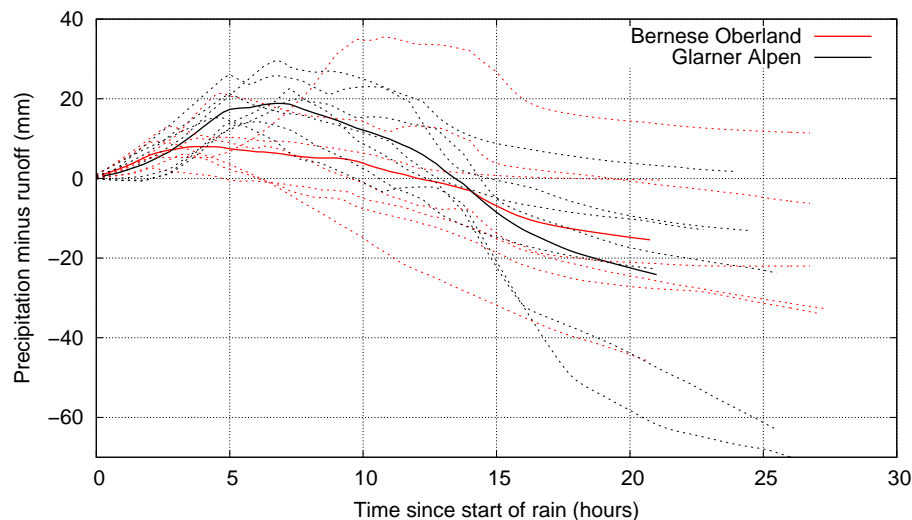


**Fig. 4.** Cumulative rainfall minus cumulative snowpack runoff during the event, starting at the onset of rain for each individual station (dashed lines) and for area averages (solid lines).

[Title Page](#)[Abstract](#)[Introduction](#)[Conclusions](#)[References](#)[Tables](#)[Figures](#)[⏪](#)[⏩](#)[◀](#)[▶](#)[Back](#)[Close](#)[Full Screen / Esc](#)[Printer-friendly Version](#)[Interactive Discussion](#)

## Simulating snow cover in rain-on-snow event

N. Wever et al.

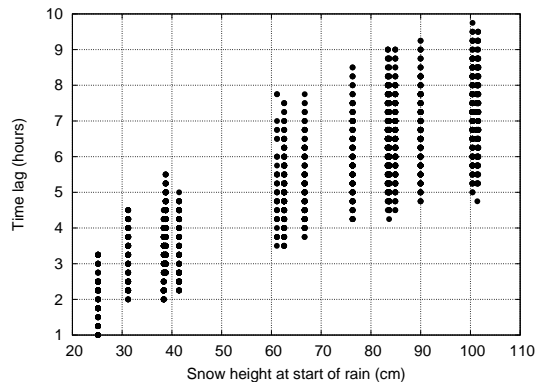


**Fig. 5.** Time lag between the start of rain and the start of snowpack runoff in hours as a function of the snow height at the onset of rain for the ensemble simulations.

[Title Page](#)[Abstract](#)[Introduction](#)[Conclusions](#)[References](#)[Tables](#)[Figures](#)[◀](#)[▶](#)[◀](#)[▶](#)[Back](#)[Close](#)[Full Screen / Esc](#)[Printer-friendly Version](#)[Interactive Discussion](#)

## Simulating snow cover in rain-on-snow event

N. Wever et al.

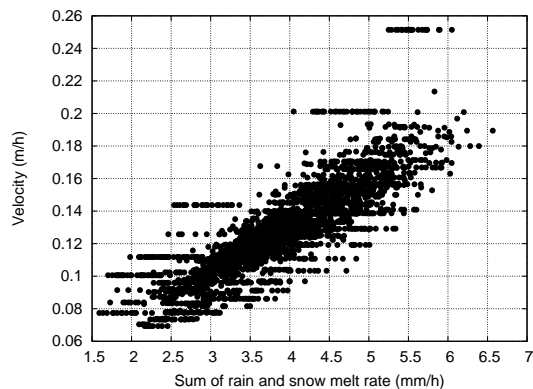


**Fig. 6.** Water velocity in the snow cover as a function of the sum of rain and snow melt in the first 5 h since the start of rain for the ensemble simulations.

[Title Page](#)[Abstract](#)[Introduction](#)[Conclusions](#)[References](#)[Tables](#)[Figures](#)[◀](#)[▶](#)[◀](#)[▶](#)[Back](#)[Close](#)[Full Screen / Esc](#)[Printer-friendly Version](#)[Interactive Discussion](#)

## Simulating snow cover in rain-on-snow event

N. Wever et al.

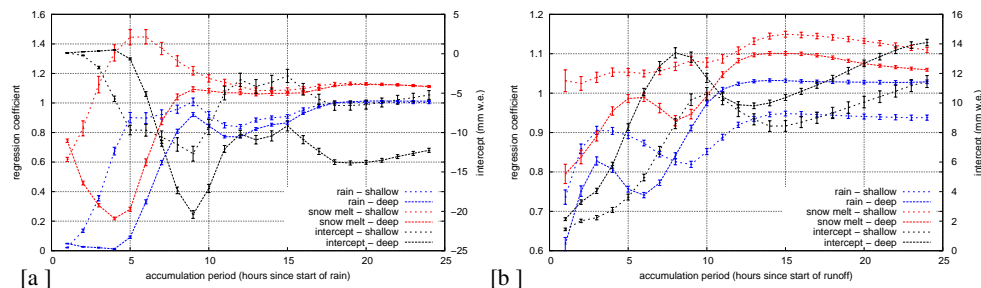


**Fig. 7.** Regression coefficients as a function of cumulative period, since the start of rain **(a)** or start of snowpack runoff **(b)**, for rain, snow melt and the intercept (mm w.e.) for both the shallow and deep snow cover class.

[Title Page](#)
[Abstract](#)
[Introduction](#)
[Conclusions](#)
[References](#)
[Tables](#)
[Figures](#)
[⏪](#)
[⏩](#)
[◀](#)
[▶](#)
[Back](#)
[Close](#)
[Full Screen / Esc](#)
[Printer-friendly Version](#)
[Interactive Discussion](#)


## Simulating snow cover in rain-on-snow event

N. Wever et al.

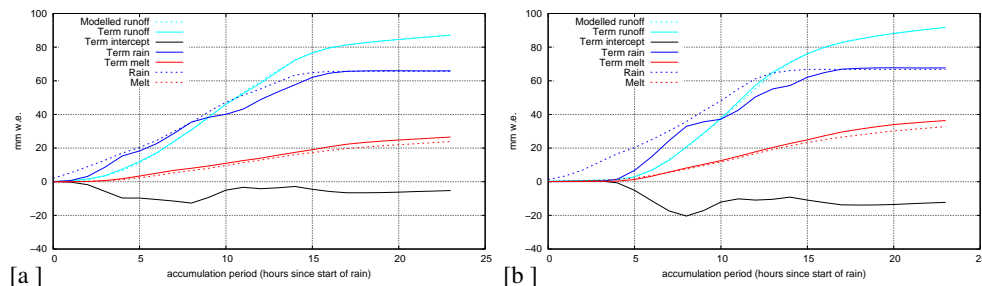


**Fig. 8.** Modelled snowpack runoff, measured rainfall and modelled snow melt together with the terms of the linear regression for both the shallow **(a)** and the deep **(b)** snow cover class. Note that the blue, red and black solid lines sum up to the cyan line.

Title Page

Abstract

Introduction

Conclusions

References

Tables

Figures

◀

▶

◀

▶

Back

Close

Full Screen / Esc

Printer-friendly Version

Interactive Discussion



## Simulating snow cover in rain-on-snow event

N. Wever et al.

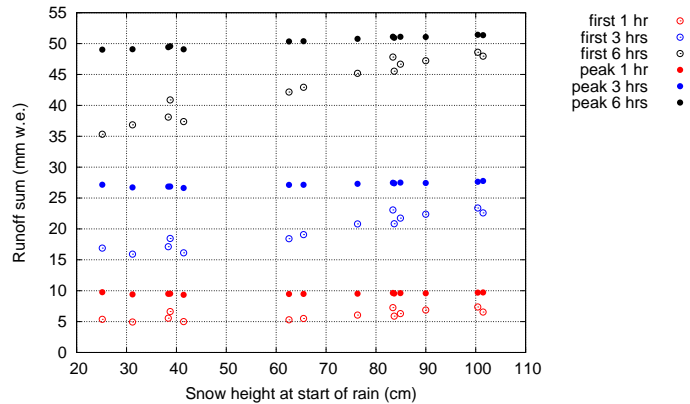


**Fig. 9.** Average maximum cumulative snowpack runoff (denoted peak) and average cumulative snowpack runoff in the first hours after the start of snowpack runoff (denoted first), averaged over all ensemble simulations.

Title Page

Abstract

Introduction

Conclusions

References

Tables

Figures

◀

▶

◀

▶

Back

Close

Full Screen / Esc

Printer-friendly Version

Interactive Discussion



